

Ion and electron emission from silver nanoparticles in intense laser fields

T. Döppner, Th. Fennel, P. Radcliffe, J. Tiggesbäumker, and K.-H. Meiwes-Broer

Institut für Physik, Universität Rostock, 18051 Rostock, Germany

(Received 7 October 2005; published 15 March 2006)

By a comparative analysis of the emission of highly charged ions and energetic electrons the interaction dynamics of intense femtosecond laser fields (10^{13} – 10^{14} W/cm²) with nanometer-sized silver clusters is investigated. Using dual laser pulses with variable optical delay the time-dependent cluster response is resolved. A dramatic increase both in the atomic charge state of the ions and the maximum electron kinetic energy is observed for a certain delay of the pulses. Corresponding Vlasov calculations on a metal cluster model system indicate that enhanced cluster ionization as well as the generation of fast electrons coincide with resonant plasmon excitation.

DOI: [10.1103/PhysRevA.73.031202](https://doi.org/10.1103/PhysRevA.73.031202)

PACS number(s): 36.40.Gk, 52.50.Jm, 33.60.-q, 31.15.Qg

The availability of intense optical lasers has fueled enormous interest in the strong-field response of various targets ranging from atoms to dense plasmas. Among those, atomic clusters are extraordinary objects since they exhibit bulk-like density within a nanometer-sized volume. Stimulated by various experimental observations the investigation of clusters in strong laser fields has grown to a rich field of current research. Early measurements on rare-gas clusters observe extremely high charged [1] and energetic ions [2,3] as well as hard X-ray emission [4] due to efficient absorption of laser light [5,6]. Shao *et al.* found direct evidence of energetic electron emission from Xe_N clusters [7] and reported on an electron energy distribution up to 3 keV that exhibited features with different angular distribution properties. More recent measurements [8,9] support the emission of keV electrons but have not verified the structured spectrum reported in Ref. [7]. Even though there is some evidence for thermal emission [8] the mechanism responsible for the generation of such energetic electrons is still under discussion. Whereas most of the results have been obtained with rare-gas clusters also experiments on metal clusters yielded fast [10,11] and highly charged ions [12]. For both, large rare-gas [13,14] and metal clusters [15,16], simulations support that resonant collective electron excitations play a crucial role for enhanced laser absorption and subsequent ionization. However, despite many theoretical models for the description of the laser-cluster interaction the exact nature of the many-body excitation and in particular its influence on the electron emission spectra as analyzed here is not fully understood yet [2,15–22].

This paper concentrates on metal clusters exposed to intense laser fields. In contrast to rare-gas systems, they exhibit delocalized electrons already in their ground state that boost many-particle effects. In a recent paper we discussed the strong influence of resonant collective electron excitation as a key to control the yield of highly charged atomic ions [23]. In the present contribution we extend this analysis and incorporate the dynamics of the electron emission from metal clusters in intense fields. Since the laser field directly couples to the electronic system, studying the electron emission appears to be promising to gain deeper insight into the laser cluster interaction process. Even though our experiments are performed at significantly lower laser intensities compared to

the measurements in Refs. [7–9] we observe energetic electrons, too. To narrow the possible mechanisms responsible for the generation of fast electrons we study the dynamics of the electron emission using dual pulses which have been proven as an efficient tool to control cluster dynamics [6,23,24]. As a reference, the dynamics in the electron emission is compared to the dynamics of the ions emerging from the Coulomb explosion. In addition, for a qualitative discussion of the observed dual-pulse spectra semiclassical Vlasov calculations on a simplified model system are performed.

Experimental details of the cluster generation, the laser system, and the detection of ionic fragments are described elsewhere [25]. In brief, silver nanoparticles having a mean radius of about 4.5 nm ($N \approx 22\,000$) are produced in a home-built magnetron gas aggregation source. A 30 Hz Ti:sapphire chirped pulse amplification system delivers 100 fs laser pulses at 800 nm. Dual pulses with an adjustable delay Δt and a typical energy of 2.5 mJ are generated by a Mach-Zehnder interferometer. The laser intensity in the interaction volume is controlled by the position of a 40 cm focusing lens with respect to the cluster beam axis. Both the charge state of emitted atomic ions as well as the kinetic electron distributions are measured by time-of-flight (TOF) methods. A reflectron mass spectrometer is used to analyze the ionic fragments. The electrons are collected by a magnetic bottle-type spectrometer with the axis perpendicular to the laser polarization. The signal detected at the channeltron is amplified and recorded by a GHz multiscaler card (FAST ComTec) having a time resolution of 0.5 ns. Each of the detector systems is located in a separate vacuum chamber on the cluster beam axis 35 to 70 cm downstream the cluster source.

Upon irradiation of the silver nanoparticles with only one of the laser pulses at 8.0×10^{13} W/cm² atomic ions up to Ag^{3+} are identified in the TOF spectrum (see Fig. 1). When additionally irradiating with the second pulse a dramatic increase both in the ion yield and the charge state can be reached. As already seen in earlier measurements [23,25] the optical delay plays a significant role in the charging process. Under the chosen cluster size and laser intensity conditions the optical delay which maximizes the charging is $\Delta t_{opt} = 4.5$ ps. The resulting charge state distribution at least extends up to Ag^{15+} (see Fig. 1). Before details of the delay

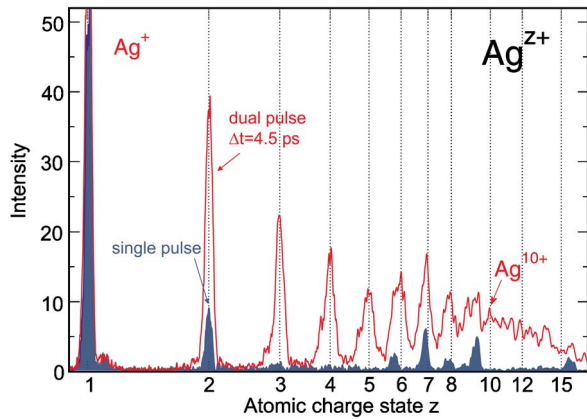


FIG. 1. (Color online) Charge state distribution of atomic ions from the Coulomb explosion of free silver nanoparticles irradiated with laser pulses of a peak intensity of 8.0×10^{13} W/cm². With an optimized optical delay of $\Delta t = 4.5$ ps the detected atomic charge state increases up to $z = 15$. Blocking one of the pulses produces Ag ions with only $z \leq 3$ (filled signal). Note, that in the range of high z the signal is superposed by contributions from residual gas.

dependence will be discussed we present data for the corresponding electron emission which was analyzed by time-of-flight measurements. Figure 2 compares the onsets of two electron TOF spectra upon single pulse (squares) and dual pulse excitation (circles), respectively. The feature at zero flight time corresponds to VUV emission and XUV emission from the excited clusters. It can be utilized to cross check the temporal offset of the time-of-flight measurements. The signals at longer flight times will not be considered here because of saturation effects at the detector. Therefore, only the highest electron energy E_{\max} , determined by the intersection of the fitted signal with an arbitrarily chosen threshold of 0.01 electrons per laser shot, is used for further data analysis. Obviously the application of the second pulse leads to a dramatic shift of E_{\max} from 75 to 375 eV. Furthermore, a strong influence of the pulse separation on E_{\max} is observed. This delay dependence is presented in Fig. 3 for two different laser intensities (dots). In order to gain deeper insight into the excitation process this dynamics is compared to the delay dependence of the ion emission. The dual pulse signal of the highest charged ions yields the most characteristic information about the interaction process [25]. Therefore we choose Ag^{10+} as a measure for the emission of highly charged ions, since it can be analyzed with sufficient statistics under the laser intensity conditions used, see diamonds in Fig. 3. Both E_{\max} and the signal of Ag^{10+} exhibit a strong variation with the pulse delay and a sharp minimum around $\Delta t = 0$ ps. With increasing delay the ion intensity and the electron energy grow rapidly and fall off slowly beyond a distinct maximum. A clear pump-probe effect can be observed up to optical delays of 100 ps. It is striking that both the ion and electron signals are maximized nearly simultaneously, see dashed vertical lines in Fig. 3. The coincidence in the maxima of the profiles persists also for other laser intensities although the optimum delay Δt_{opt} differs. Thus the particular value of Δt_{opt} which is roughly 5 ps for 8.0×10^{13} W/cm² and 12 ps for 2.5×10^{13} W/cm² appears to be a function of the laser

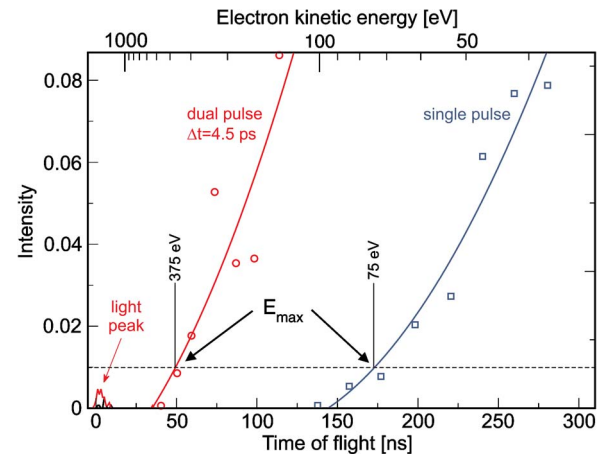


FIG. 2. (Color online) Onsets of electron time-of-flight spectra from Ag particles upon irradiation with single (squares) and dual pulses ($\Delta t = 4.5$ ps, circles) of 8×10^{13} W/cm². The corresponding electron energies are depicted at the top. The feature at zero flight time corresponds to light emission. Intersections of the fit functions with a threshold (dashed horizontal line) define the maximum electron energy E_{\max} .

intensity. In previous studies on the ion emission [23,25] it has already been shown that the laser power influences the interaction process in two ways: Firstly, the higher the laser intensity the shorter the optimum delay Δt_{opt} . Secondly, with a higher intensity the second pulse applied with the optimum delay yields a more efficient charging of the clusters. Also the latter trend finds its correspondence in the maximum electron energy E_{\max} which increases from 265 eV at 2.5×10^{13} W/cm² to 375 eV at 8.0×10^{13} W/cm².

Thus it is suggestive to assume a connection of the mechanisms responsible for the enhancement in the electron energies and the yield of highly charged ions. Previously, the model of plasmon enhanced ionization was considered [12,23] to explain the significantly increased yield of highly charged ions for a certain delay. Its particular value is determined by the expansion of the pre-excited cluster to the critical radius which leads to a matching between the spectral position of the dipole plasmon and the laser photon energy. Since a resonant collective excitation is associated with strong laser absorption more energy is available to release electrons expressed by an enhanced yield of highly charged fragments. Hence a stronger excitation can explain a higher number of emitted electrons, but not necessarily significantly higher kinetic energies. It should be noted that ponderomotive effects [26] are by far not sufficient to account for the observed energies. The ponderomotive potential which is defined by the mean kinetic energy of a free electron in the laser field reaches only 4.8 eV for the highest laser intensity used in this study. Since direct multiphoton absorption is also unlikely to be important for the high energy tail of the electron spectrum when using a laser photon energy of 1.5 eV a more complex emission process seems to be present.

A deeper insight into the laser cluster interaction can be gained by time-dependent microscopic models which have already been proven to be able to explain the charging dynamics in metal clusters [23]. In order to investigate the as-

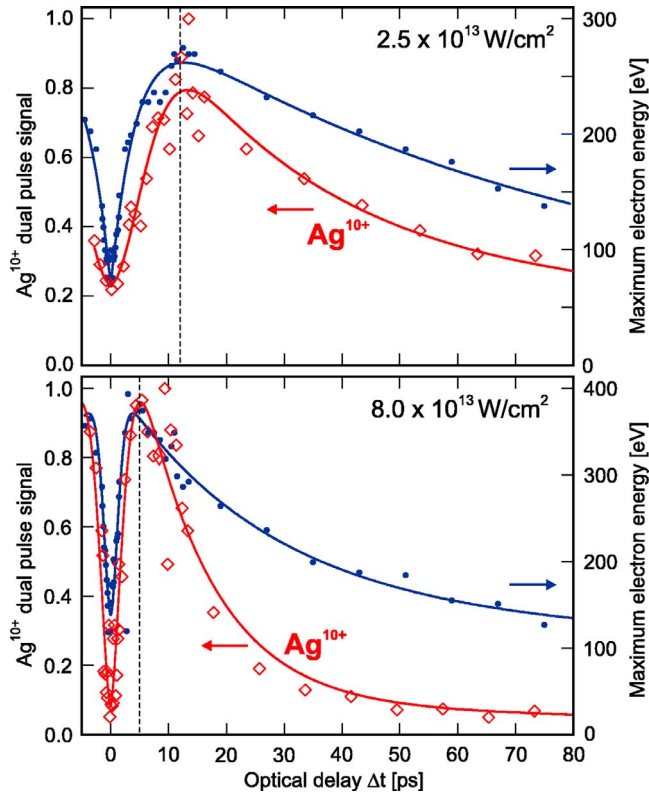


FIG. 3. (Color online) Comparison of the Ag^{10+} yield (diamonds, left axis) with the maximum kinetic energy E_{max} of the emitted electrons (dots, right axis) following dual pulse excitation of large Ag_N at a laser intensity of $2.5 \times 10^{13} \text{ W/cm}^2$ (upper panel) and $8.0 \times 10^{13} \text{ W/cm}^2$, respectively. The lines are guide to the eye fits. Both the electron and the ion signals exhibit a strong dynamics and their maxima occur nearly simultaneously (see dashed vertical lines), irrespective of the laser intensity.

sociation of the emission of fast electrons to collective excitations in more detail, numerical simulations have been performed on a simplified model system of metal clusters, i.e., Na_{55} . For the description of the laser-cluster interaction we use Thomas-Fermi-Vlasov molecular dynamics (TFV-MD) which provides a semiclassical treatment of valence electrons coupled to classically propagated atomic ions via local pseudopotentials. Details of the theoretical approach and the numerical methods are described elsewhere [16,23]. In the present study we extended the model to a considerably larger simulation box and additionally calculate the energy spectra of emitted electrons. In the analysis we concentrate on the comparison of the average charge state of emitted ions to the highest kinetic energy of emitted electrons. Results for a set of simulations considering a dual-pulse excitation with 50 fs Gaussian pulses at $I_0 = 4 \times 10^{12} \text{ W/cm}^2$ are given in Fig. 4. The average ionization (circles) exhibits a pronounced maximum if the second pulse irradiates the cluster with a delay of 275 fs, exactly when the energy of the collective dipole mode matches the laser photon energy [23], see dotted vertical line. For both, shorter and longer optical delays the ionization is significantly lowered. Although the simulations yield different time scales and absolute numbers, the overall structure of the de-

lay dependence is in agreement with the experimental observations, and also with measurements on small metal clusters [23,25]. As an additional result of our calculations the corresponding maximum kinetic energies of emitted electrons (squares) are plotted in Fig. 4. They follow the same trend as the experimental data shown in Fig. 3, i.e., for an optimum delay the electron energy is significantly enhanced. Moreover, the optimum coincides with the resonant excitation which makes us confident that the simulations qualitatively reproduce the delay dependence of the electron emission process. Similar to the experimental results the maximum electron energies greatly exceed the ponderomotive potential which is $U_p = 0.24 \text{ eV}$ for the calculated scenario. Whereas the ratio E_{max}/U_p is between 80 and 180 for the experiments, a value of 63 was found in the simulations. For comparison, in the experiments on rare-gas cluster values between 4 [7] and ≈ 20 [8,9] were obtained. Since electron-electron collisions are not included in the simulations at this point, the enhancement cannot be due to the high energy tail of a thermal energy spectrum of the electrons. Especially at the optimum delay the energy spectrum has a strong nonthermal character (not shown here). For that reason we assume a dynamical mechanism for electron acceleration that is directly connected to plasmon enhanced absorption instead of a simple thermal emission at a higher temperature.

In conclusion, we report on the emission of energetic electrons from large metal clusters under strong dual-pulse excitation. The measured kinetic energy greatly exceeds that which is expected from ponderomotive effects. The measurements indicate a drastic enhancement for the emission of fast electrons for an optimum delay that coincides with the generation of highly charged ions. This strong association is also found in the results from numerical simulations which support a nonthermal origin for the high-energy tail of the spectrum. Since the experiments are performed with a size distribution, an even stronger dynamics is expected when probing

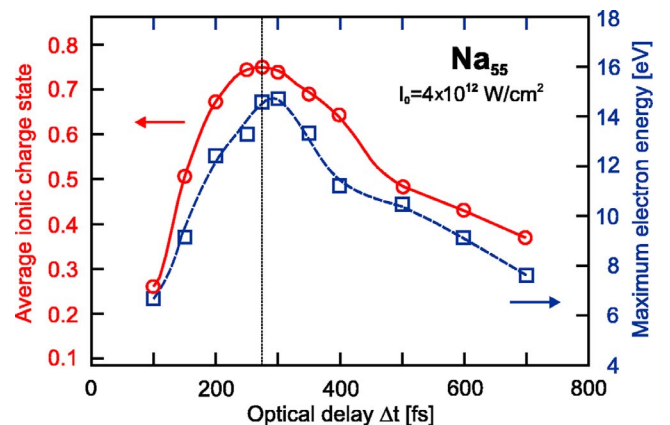


FIG. 4. (Color online) Calculated average ionic charge state (circles, left axis) and maximum energy of emitted electrons (squares, right axis) resulting from the irradiation of Na_{55} with two 50 fs laser pulses ($I_0 = 4 \times 10^{12} \text{ W/cm}^2$, $\lambda = 800 \text{ nm}$) in dependence of their optical delay Δt . Both the ionization and the electron energy are maximized at $\Delta t = 275 \text{ fs}$ for which the second pulse resonantly excites the collective electron dipole mode of the cluster (vertical dashed line).

size selected clusters. The exact nature of the acceleration mechanism that produces the energetic electrons remains an open question. Further investigations to clarify the detailed structure of the electron emission spectra including the angular distribution are subjects of current experimental and theoretical research.

The authors gratefully acknowledge financial support by the Deutsche Forschungsgemeinschaft within the Sonderforschungsbereich 652. Furthermore, we like to thank the German Verbund für Hoch- und Höchstleistungsrechnen Nord (HLRN) for providing computer resources for the calculations.

-
- [1] E. M. Snyder, S. A. Buzza, and A. W. Castleman Jr., *Phys. Rev. Lett.* **77**, 3347 (1996).
- [2] T. Ditmire, J. W. G. Tisch, E. Springate, M. B. Mason, N. Hay, J. P. Marangos, and M. H. R. Hutchinson, *Phys. Rev. Lett.* **78**, 2732 (1997).
- [3] E. Springate, N. Hay, J. W. G. Tisch, M. B. Mason, T. Ditmire, M. H. R. Hutchinson, and J. P. Marangos, *Phys. Rev. A* **61**, 063201 (2000).
- [4] A. McPherson, B. D. Thompson, A. B. Borisov, K. Boyer, and C. K. Rhodes, *Nature (London)* **370**, 631 (1994).
- [5] T. Ditmire, R. A. Smith, J. W. G. Tisch, and M. H. R. Hutchinson, *Phys. Rev. Lett.* **78**, 3121 (1997).
- [6] J. Zweiback, T. Ditmire, and M. D. Perry, *Phys. Rev. A* **59**, R3166 (1999).
- [7] Y. L. Shao, T. Ditmire, J. W. G. Tisch, E. Springate, J. P. Marangos, and M. H. R. Hutchinson, *Phys. Rev. Lett.* **77**, 3343 (1996).
- [8] V. Kumarappan, M. Krishnamurthy, and D. Mathur, *Phys. Rev. A* **67**, 043204 (2003).
- [9] E. Springate, S. A. Aseyev, S. Zamith, and M. J. J. Vrakking, *Phys. Rev. A* **68**, 053201 (2003).
- [10] S. Teuber, T. Döppner, Th. Fennel, J. Tiggesbäumker, and K.-H. Meiwes-Broer, *Eur. Phys. J. D* **16**, 59 (2001).
- [11] M. A. Lebeault, J. Viallon, J. Chevalere, C. Ellert, D. Normand, M. Schmidt, O. Sublemontier, C. Guet, and B. Huber, *Eur. Phys. J. D* **20**, 233 (2002).
- [12] L. Köller, M. Schumacher, J. Köhn, S. Teuber, J. Tiggesbäumker, and K.-H. Meiwes-Broer, *Phys. Rev. Lett.* **82**, 3783 (1999).
- [13] T. Ditmire, T. Donnelly, A. M. Rubenchik, R. W. Falcone, and M. D. Perry, *Phys. Rev. A* **53**, 3379 (1996).
- [14] U. Saalmann and J.-M. Rost, *Phys. Rev. Lett.* **91**, 223401 (2003).
- [15] P.-G. Reinhard and E. Suraud, *Appl. Phys. B* **73**, 401 (2001).
- [16] Th. Fennel, G. F. Bertsch, and K.-H. Meiwes-Broer, *Eur. Phys. J. D* **29**, 367 (2004).
- [17] C. Rose-Petruck, K. J. Schafer, K. R. Wilson, and C. P. J. Barty, *Phys. Rev. A* **55**, 1182 (1997).
- [18] K. Ishikawa and T. Blenski, *Phys. Rev. A* **62**, 063204 (2000).
- [19] Ch. Siedschlag and J.-M. Rost, *Phys. Rev. Lett.* **89**, 173401 (2002).
- [20] Ch. Jungreuthmayer, M. Geissler, J. Zanghellini, and Th. Bräbäck, *Phys. Rev. Lett.* **92**, 133401 (2004).
- [21] J. Daligault and C. Guet, *Phys. Rev. A* **64**, 043203 (2001).
- [22] K. Andrae, P.-G. Reinhard, and E. Suraud, *Phys. Rev. Lett.* **92**, 173402 (2004).
- [23] T. Döppner, Th. Fennel, Th. Diederich, J. Tiggesbäumker, and K.-H. Meiwes-Broer, *Phys. Rev. Lett.* **94**, 013401 (2005).
- [24] S. Zamith, T. Martchenko, Y. Ni, S. A. Aseyev, H. G. Müller, and M. J. J. Vrakking, *Phys. Rev. A* **70**, 011201(R) (2004).
- [25] T. Döppner, Th. Fennel, P. Radcliffe, J. Tiggesbäumker, and K.-H. Meiwes-Broer, *Eur. Phys. J. D* **36**, 165 (2005).
- [26] P. B. Corkum, *Phys. Rev. Lett.* **71**, 1994 (1993).